ROS-associated mechanism of different concentrations of pinacidil postconditioning in the rat cardiac Nrf2-ARE signaling pathway

WEI CHEN[1*], MENGYUAN DENG[1*], HAIYING WANG[1], YING WANG[1], WENJING ZHOU[1] and TIAN YU[2]

[1]Department of Anesthesiology, Affiliated Hospital of Zunyi Medical University;
[2]Zunyi Medical University, Zunyi, Guizhou 563000, P.R. China

Received April 5, 2020; Accepted February 25, 2021

DOI: 10.3892/mmr.2021.12072

Abstract. Previous studies have confirmed that 50 μmol/l pinacidil postconditioning (PPC) activates the nuclear factor-E2 related factor 2 (Nrf2)-antioxidant responsive element (ARE) pathway, which protects the myocardium from ischemia-reperfusion (IR) injury; however, whether this is associated with reactive oxygen species (ROS) generation remains unclear. In the present study, a Langendorff rat model of isolated myocardial IR was established to investigate the mechanism of PPC at different concentrations, as well as the association between the rat myocardial Nrf2-ARE signaling pathway and ROS. A total of 48 rats were randomly divided into the following six groups (n=8 per group): i) Normal; ii) IR iii) 10 μmol/l PPC (P10); iv) 30 μmol/l PPC (P30); v) 50 μmol/l PPC (P50); and vi) N-(2-mercaptopropionyl)-glycine (MPG; a ROS scavenger) + 50 μmol/l pinacidil (P50 + MPG). At the end of reperfusion (T3), compared with the IR group, the P10, P30 and P50 groups exhibited improved cardiac function, such as left ventricular development pressure, heart rate, left ventricular end-diastolic pressure, +dp/dtmax, myocardial cell ultrastructure and mitochondrial Flameng score. Furthermore, the P10 and P50 groups demonstrated the weakest and most marked improvements, respectively. Additionally, in the P10, P30 and P50 groups, the residual ROS content at the end of reperfusion was highly negatively correlated with relative expression levels of Nrf2 gene and protein. Higher pinacidil concentration was associated with higher ROS generation at 5 min post-reperfusion (T2), although this was significantly lower compared with the IR group, as well as with increased expression levels of antioxidant proteins and phase II detoxification enzymes downstream of the Nrf2 and Nrf2-ARE pathways. This result was associated with a stronger ability to scavenge ROS during reperfusion, leading to lower levels of ROS at the end of reperfusion (T3) and less myocardial damage. The optimal myocardial protective effect was achieved by 50 mmol/l pinacidil. However, cardiac function of the P50 + MPG group was significantly decreased, ultrastructure of cardiomyocytes was significantly impaired and the relative expression levels of genes and proteins in the Nrf2-ARE pathway were decreased. The aforementioned results confirmed that different PPC concentrations promoted early generation of ROS and activated the Nrf2-ARE signaling pathway following reperfusion, regulated expression levels of downstream antioxidant proteins and alleviated myocardial IR injury in rats. Treatment with 50 mmol/l pinacidil resulted in the best myocardial protection.

Introduction

In 2003, Zhao *et al* (1) confirmed that in the early stages of ischemia-reperfusion (IR) injury, it is possible to achieve myocardial protection by applying repeated ischemic treatments; this process was termed ischemic postconditioning (IPO). IPO can alleviate oxidative stress, maintain endothelial function, decrease calcium accumulation and protect the heart muscle from damage (2). The mechanism of IPO relies on complex signaling pathways, involving G-protein-coupled (3) and membrane growth factor receptors and mitochondrial ATP-sensitive potassium channels (KATPs) (4). These pathways act on terminal effector mitochondrial permeability transition pores (mPTPs) to prevent pore formation, and thus serve a key role in myocardial protection (5). KATP regulates ATP levels via intracellular alterations to potassium ions concentrations. There are two types of independent KATPs in cardiomyocytes: Sarcolemmal (sarcKATP) and mitochondrial (mitoKATP), both of which are necessary for myocardial protection (6).

Pinacidil is a non-selective KATP channel opener that exhibits cardioprotective effects (7). Pinacidil opens both sarcKATP and mitoKATP channels, triggering cell membrane hyperpolarization and mitochondrial membrane depolarization, thereby decreasing myocardial ATP levels. This was confirmed by a previous study (8) using isolated rat hearts as a model to test the combination of histidine-tryptophan-ketoglutarate solution and pinacidil as an improved strategy for

Correspondence to: Professor Haiying Wang, Department of Anesthesiology, Affiliated Hospital of Zunyi Medical University, 201 Dalian Road, Huichuan, Zunyi, Guizhou 563000, P.R. China
E-mail: wanghaiting-8901@163.com

*Contributed equally

Key words: ischemia-reperfusion injury, pinacidil nuclear factor E2-related factor-antioxidation reaction pathway, reactive oxygen species

donor heart preservation. Our previous study confirmed that pinacidil postconditioning (PPC) at different concentrations inhibits IR injury in rats, primarily by upregulating nuclear factor erythroid 2-related factor 2 (Nrf2) and its downstream genes, such as NADH-quinone oxidoreductase-1 (NQO1), heme oxygenase 1 (HO-1) and superoxide dismutase 1 (SOD1), all of which serve important roles in myocardial protection (9). However, our study did not investigate the myocardial protective effects of different pinacidil concentrations or the association between pinacidil and reactive oxygen species (ROS), which are an important component in myocardial protective signaling. Furthermore, it was not determined whether different concentrations of ROS alters Nrf2, NQO1, SOD1 and HO-1 expression levels to alleviate myocardial IR injury (MIRI) (9).

Nrf2 is a member of the basic leucine zipper transcription factor cap'n'collar family, which is constitutively expressed in the cytoplasm. Its accumulation and activation in the nucleus causes oxidative damage (10). In cancer cells, Nrf2 combines with antioxidant response element (ARE) to decrease damage. Its antioxidant defense enzymes (including HO-1 and NQO1) have anti-inflammatory and anti-apoptotic functions, which can reduce oxidative stress in cells. Nrf2 usually combines with the ARE, which is the promoter region of HO-1, SOD, and NQO1, etc. (11). After combination, the enzyme complex upregulates expression of endogenous protective antioxidant genes, such as HO-1, NQO1 and SOD, in the tissue, thereby maintaining the balance of oxidant and antioxidant levels in cells (12).

Studies have shown that HO-1 is the primary endogenous protective gene regulated by the Nrf2-ARE signaling pathway (13,14). HO-1 has multiple effects, which are activated by Nrf2 and its metabolites; in particular, it can scavenge hydroxyl-free radicals, singlet oxygen, and superoxide anions to prevent oxidation of lipids. Therefore, HO-1 could play an indispensable role in the prevention of apoptosis (14).

NQO1 is a two-electron reductase, which is widely present in the cytoplasm and catalyzes the reduction of quinone substrates (15). It has been reported that NQO1 can protect cells from oxidative stress by inhibiting the reduction of semiquinone free radicals and the formation of ROS (16,17). During myocardial protection, NQO1 is induced following activation of ARE and exhibits protective effects against various metabolic oxidative stress responses (18).

SOD is one of the proteins regulated by the Nrf2-ARE signaling pathway. SOD is the primary antioxidant enzyme in and free radical scavenger in cells; thus SOD protects cells against oxygen free radicals. The levels of SOD reflect the function of the endogenous oxygen free radical scavenging system (19).

Research has confirmed that Nrf2 protect cardiomyocytes from oxidative stress by increasing detoxification pathways, enhancing antioxidant potential and alleviating oxidative damage in various disease states (20).

N-(2-mercaptopropionyl)-glycine (MPG) is a class of synthetic thiol compounds with ROS scavenging properties and exerts protective effects in MIRI (21). Studies have reported that MPG decreases heart hypertrophy of spontaneously hypertensive rats due to IRI (22,23). These effects may be associated with inhibited opening of mPTP and decreased myocardial oxidative stress. MPG can be used for oral prophylactic treatment and is approved by the United States Food and Drug Administration (FDA) for human clinical use (24).

To the best of our knowledge, it remains unknown whether ROS serve a role in PPC. Based on previous studies, pinacidil-postconditioning is considered to be equivalent to ischemic postconditioning in defeating cardiac IR injury in rats (9,22); therefore, our present study aimed to use the Langendorff device to establish an IR model in rats, and to simulate the process of cardiac arrest-relapse during surgery. Thereafter, changes in cardiac function, myocardial infarction and myocardial ultrastructure were observed, and the expression levels of Nrf2, HO1, SOD1 and other antioxidant proteins were detected. In addition, the research assessed whether different doses of pinacidil could generate different levels of ROS, activate the Nrf2-ARE pathway to different degrees and exert different effects on myocardial protection. The present study aimed to provide evidence for the potential use of pinacidil in clinical practice and the treatment of MIRI.

Materials and methods

Experimental animals. Healthy, specific-pathogen-free grade, 48 male Sprague-Dawley rats (age, 16-20 weeks; weight, 250-300 g) were purchased from the Animal Centre of DaPing Hospital, Army Military Medical University in China [certificate no. SCXK (YU) 2007-0005]. The present experiment was performed in accordance with document No. 36 of the Animal Ethics Review at The Affiliated Hospital of Zunyi Medical University in 2016. The rats were housed in individual ventilation cages and provided with food and water *ad libitum*. Rats were housed under a 12-h light/dark cycle, at 20-25˚C and 50-65% humidity. All animal experiments were performed in accordance with the U.K Animals Act of 1986, and associated guidelines EU Directive 2010/63/EU (25). Furthermore, the process of feeding rats was compliant with the National Institutes of Health: Guide for the Care and Use of Laboratory Animals (2011) (26).

Langendorff reperfusion protocol. The Langendorff reperfusion protocol was performed as described previously (9). The rats were intraperitoneally injected with 1% pentobarbital solution (35 mg/kg) and heparin (250 U/kg). The xiphoid process was marked and the upper abdomen was cut horizontally along both sides of the costal margin to expose the diaphragm. The thoracic cavity was cut on the cephalic side through the midline of both sides of the iliac crest. The xiphoid process was lifted with tweezers to open the thoracic cavity and expose the heart. Finally, the heart was removed and separated from the roots along with the aorta and quickly placed in pre-cooled (4˚C) Krebs-Henseleit (K-H) buffer (in mM: 118 NaCl, 25 $NaHCO_3$, 4.8 KCl, 1.2 KH_2PO_4, 1.19 MgCl, 2.6 H_2O, 1.2 $MgSO_4$, 2.5 $CaCl_2$, and 11.110 glucose; pH 7.4) to clean and wash away the blood.

The aorta was fixed on a Langendorff system perfusion needle (Panlab), which was prefilled with K-H solution and retrogradely perfused. The K-H solution (gassed with 95% O_2 and 5% CO_2) was heated to 37˚C. The solution was infused and connected to PowerLab physiological experiment equipment (ADInstruments, Ltd.) to test the pressure. The pulmonary

artery root was incised to improve the right ventricular flow. A small orifice was created at the left atrial appendage and a latex balloon was placed into the mitral valve to collect data on cardiac function. The balloon was adjusted to maintain a left ventricular end-diastolic pressure (LVEDP) of 2-5 mmHg. Throughout the perfusion process, the K-H solution was maintained at room temperature to sustain the heartbeat and regulate the perfusion pressure, which was stabilized at 60-70 mmHg.

After K-H solution had equilibrated at 37˚C for 20 min (time point T1), the left ventricular developed pressure (LVDP) and heart rate (HR) were assessed. The experiment was allowed to continue if LVDP >80 mmHg, HR >250 beats/min and ventricular premature beat <2 times; if these conditions were not met, the experiment was terminated.

At the end of balanced perfusion (T1), the isolated hearts were randomly divided into the following six groups (n=8/group): Normal (N) group, hearts were perfused with K-H solution for a further 180 min; IR group, hearts underwent ischemia for 40 min, followed by 120 min reperfusion; P10, P30 and P50 groups, hearts underwent ischemia for 40 min followed by 10, 30, and 50 μmol/l pinacidil treatment, respectively, for 2 min prior to reperfusion with K-H solution for 118 min; and M + P50 group, hearts underwent ischemia for 40 min followed by treatment with 50 μmol/l pinacidil for 2 min, then treatment with K-H solution containing 2 mmol/l ROS scavenger MPG (Sigma-Aldrich; Merck KGaA) for 3 min and reperfusion with K-H solution for 115 min. The experimental procedure for each group is presented in Fig. 1.

T2 was defined as 5 min post-reperfusion and T3 was defined as the end of reperfusion. At T1 and T3, PowerLab physiological experiment equipment (ADInstruments Ltd.) was used to collect data on cardiac function indicators, such as HR, LVDP, LVEDP and the maximal rate of rise in blood pressure in the ventricular chamber (+dP/dtmax).

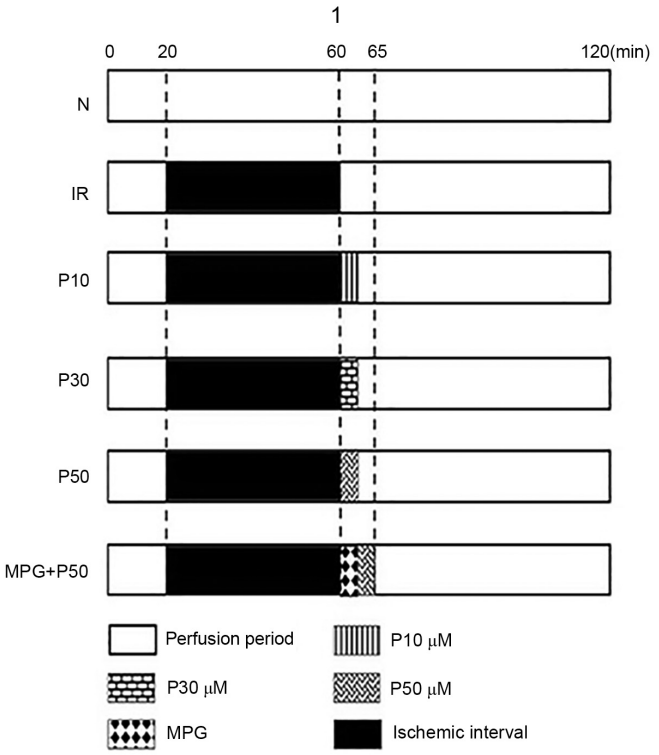

Figure 1. Grouping strategy and perfusion measures in rats. Rats were allocated to six groups (n=8/group): N, IR, P10, P30, P50 and MPG + P50. In the N group, hearts were perfused with K-H solution for 180 min. The other rat hearts were equilibrated for ≥20 min (during which the flow was adjusted to a mean perfusion pressure of 60-70 mmHg). In the IR group, hearts underwent ischemia (perfusion was paused) for 40 min, followed by 120 min reperfusion. In the P10, P30 and P50 groups, hearts underwent 40 min of ischemia followed by treatment with 10, 30, and 50 μmol/l pinacidil, respectively, for 2 min, and reperfusion for 118 min. In the M + P50 group, hearts underwent ischemia for 40 min followed by treatment with 50 μmol/l pinacidil for 2 min and K-H solution containing 2 mmol/l ROS scavenger MPG for 3 min, then reperfusion with K-H solution for 115 min. N, normal; IR, ischemia-reperfusion; MPG, N-(2-mercaptopropionyl)-glycine; K-H, Krebs-Henseleit; P10, 10 μmol/l pinacidil; P30, 30 μmol/l pinacidil; P50, 50 μmol/l pinacidil.

Ultrastructural observation of myocardial tissue and mitochondrial Flameng score. A pre-cooled (4˚C) 2.5% glutaraldehyde electron microscope fixative was prepared. Next, 0.1-cm^2 pieces of myocardial tissue were excised from the left ventricle at T3 (the entire process was completed in ≤1 min) and placed in the 4˚C precooled 2.5% glutaraldehyde fixative (for no more than 2 weeks). The tissue samples were then rinsed three times with phosphate buffer (every 2 h). Subsequently, the tissue samples were placed in pre-cooled (4˚C) 1% citric acid for 2 h. Finally, the tissue samples were dehydrated using ethanol and acetone gradients and embedded in epoxy resin at 45˚C for 12 h and 60˚C for 48 h, which was allowed to polymerize, before double staining with uranyl acetate at 20-25˚C for 20 min and lead citrate at 20-25˚C for 10 min. The ultrastructure of the myocardial tissue was then observed using a transmission electron microscope (Hitachi H7500) (magnification, x20,000) and the mitochondrial Flameng score was determined.

The specific criteria for determining the mitochondrial Flameng score based on transmission electron microscopy were as previously described (27). In brief, five fields of view (each containing 20 mitochondria) were randomly selected for each tissue slice. The mitochondrial Flameng score (range, 0-4) for each group was expressed as the mean ± SD. Flameng score increases with damage to the myocardial mitochondrial (28).

Reverse transcription-quantitative (RT-q)PCR. At T3, total RNA was isolated from the myocardial tissue using a Takara RNA Iso Plus kit (Takara Bio, Inc.). The RNA concentration and purity were measured using a microplate reader to assess the optical density (OD) at 260 and 280 nm of each sample. RNA samples meeting the purity standards (OD260/OD280, 1.8-2.1) were diluted and used to assess relative expression levels of Nrf2, HO-1, SOD1 and NQO1. GAPDH was used as a control. The primer sequences for each gene were as follows: Nrf2 forward, 5'-TTGGCAGAGACATTCCCATTTGTA-3' and reverse, 5'-ATCAGTCATGGCCGTCTCCAG-3'; HO-1 forward, 5'-AGGTGCACATCCGTGCAGAG-3' and reverse, 5'-TCCAGGGCCGTATAGATATGGTACA-3'; SOD1 forward, 5'-AATGTGTCCATTGAAGATCGTGTGA-3' and reverse, 5'-GCTTCCAGCATTTCCAGTCTTTGTA-3'; GAPDH forward, 5'-GGCACAGTCAAGGCTGAGAATG-3' and reverse 5'-ATGGTGGTGAAGACGCCAGTA-3'; and NQO1 forward, 5'-TGGAAGCTGCAGACCTGGTG-3' and reverse, 5'-TTGTCATACATGGTGGCATACGTG-3'.

After preparing each pair of target gene primers, the reaction system was configured and a Takara RT-qPCR kit was used to perform the reaction according to the manufacturer's instructions. If a single peak appeared in the dissolution curve of the PCR target gene, the target gene results were considered specific and were quantitatively analyzed, using the Cq value as a comparative statistic (29). Finally, the expression of each gene relative to the internal reference GAPDH gene was determined.

Western blotting. At T3, left ventricular tissue with a net weight of 50 mg was obtained and added to a 1.5-ml Eppendorf tube containing RIPA buffer (high efficiency) (Beijing Solarbio Science & Technology Co., Ltd.) (sample:buffer, 50 mg: 1 ml. The total protein level in the tissue was then quantified using a bicinchoninic acid protein concentration assay kit (Beijing Solarbio Science & Technology Co., Ltd.). The protein concentrations were calculated according to a standard curve. Following denaturation at 100˚C for 5 min, the proteins were cooled to room temperature and centrifuged (12,000 x g, 4˚C, 2 min). Equivalent amounts of protein (40 μg/lane) from each group were separated by SDS-PAGE (10% separating gel; 4% stacking gel), transferred onto polyvinylidene fluoride (PVDF) membranes and blocked with western blocking buffer (Beijing Solarbio Science & Technology Co., Ltd.) at room temperature for 2 h. The membranes were then incubated at 4˚C overnight with primary antibodies (Nrf2, 1:1,000, cat. no. ab62352; NQO1, 1:1,000, cat. no. ab79694; HO-1, 1:250, cat. no. ab137749; SOD1, 1:1,000, cat. no. ab13498; all Abcam), using GAPDH (1:3,000, cat. no. ab181602, Abcam) as the internal reference. Membranes were incubated with a secondary antibody (1:3,000, cat. no. SE134; Beijing Solarbio Science & Technology Co., Ltd.) for 1 h at room temperature and then washed twice in TBS-0.1% Tween (Abcam). Finally, each membrane was scanned using an infrared fluorescence imaging system with ECL Western Blotting Substrate (Beijing Solarbio Science & Technology Co., Ltd.). The PVDF membranes were scanned and detected using ChemiDoc Imaging system (Bio-Rad Laboratories, Inc.).

ROS level detection. Samples of left ventricular muscle tissue (100 mg) were taken at T2 and T3. The Fluorometric Intracellular ROS Kit (cat. no. MAK144-1KT; Sigma-Aldrich, Inc.) was then used to calculate the concentration of ROS in each sample based on a standard curve.

Statistical analysis. Statistical analysis was performed using SPSS 18.0 statistical software for Windows (IBM Corp.). For myocardial morphology and Flameng score, the Kruskal-Wallis test was used to assess myocardial damage, with Dunn's post hoc test. Gene and protein expression levels in isolated rat hearts at T3 with a normal distribution are presented as the mean ± SD (n=3). Significance of differences between the six groups was determined by one-way ANOVA followed by post hoc Bonferroni's correction. Welch's ANOVA was used when variance was not uniform. Scatter plots of ROS and Nrf2 gene/protein levels at T3 were assessed by Pearson correlation analysis. For ROS levels at T2 and T3 in each group, two-way ANOVA was used, with time as the independent factor. Bonferroni's correction was performed as a post hoc test. $P<0.05$ was considered to indicate a statistically significant difference.

Results

Different concentrations of PPC decrease MIRI to varying degrees. At T3 (end of reperfusion), the cardiac function of the IR group was significantly decreased (HR, LVDP and +dp/dtmax were decreased, whereas LVEDP was increased), suggesting impaired left ventricular function.

The LVDP, LVEDP and +dp/dtmax of the IR myocardium were restored in the P10, P30 and P50 groups, and recovery in the P50 group was the most notable. The HR, LVDP and +dp/dtmax of the M + P50 group were decreased and LVEDP was increased compared with the P50 group (Table I).

Compared with T1, there was a significant difference in HR, LVDP, LVEDP and +dp/dtmax in the P10 and P30 groups at T3. However, the P50 group showed no significant difference (Table I).

Different concentrations of PPC decrease myocardial ultrastructural damage in IR (Fig. 2A and B). The ultrastructure of cardiomyocytes was normal at the end of reperfusion in the N group. The IR group exhibited the most severe damage, cell edema, disordered myofilaments and ruptured nuclear membrane. Mitochondria were notably swollen with vacuolar degeneration. In the P10 and P30 groups, the myofilaments were arranged neatly, the sarcoplasmic reticulum was dilated, part of the mitochondria was swollen and the structure was clear but intermittently dissolved and broken. In the P50 group, the myocardial cell structure was more complete compared with the IR group, the myofilaments were neatly arranged, the Z line and the sarcomere were clearly visible, the mitochondria were structurally intact and arranged neatly and the sarcoplasmic reticulum was slightly expanded. In the M + P50 group, the myocardial cell structure was more severely damaged compared with in the P50 group, the myofilaments and Z-line were broken, the mitochondrial structure was intact but slightly swollen and the sarcoplasmic reticulum was slightly expanded, as compared with in the P50 group.

Different concentrations of PPC maintain myocardial mitochondrial structural integrity in IR. At T3, the mitochondrial structure of myocardial tissue in the N group was normal and the Flameng score was the lowest (Fig. 2B). The IR group score was the highest, suggesting most severe mitochondrial damage. The mitochondrial Flameng scores of the P10, P30 and P50 groups were all lower compared with the IR group; the P50 group had the lowest score. As the score of the M + P50 group was higher than that of the P50 group, this was suggestive of aggravated damage (Fig. 2B).

RT-qPCR analysis of relative expression levels of Nrf2, HO-1, NQO1 and SOD-1 in myocardial tissue at T3. At T3, the relative mRNA expression levels of Nrf2, HO-1, NQO1 and SOD1 were significantly decreased in the IR group compared with the N group (Fig. 3). Compared with the IR group, the relative mRNA expression levels in the P10, P30 and P50 groups were significantly increased. Among all groups, the relative expression levels of Nrf2, HO-1, NQO1 and SOD1 were highest in

Table I. Changes in HR, LVEDP, LVDP and +dP/dtmax in each group at T1 and T3. Compared with the N group, the cardiac function of the IR group was significantly impaired.

	HR, beats/min		LVEDP, mmHg		LVDP, mmHg		+dp/dtmax, mmHg	
Group	T1	T3	T1	T3	T1	T3	T1	T3
N	318±13	311±17	5±1	5±1	108±8	99±4	4,589±257	3,779±387
IR	295±17	225±59[a]	5±1	20±3[a]	103±23	53±16[a]	4,455±149	2,172±480[a]
P10	298±19	250±41[b]	4±2	8±6[b]	115±16	70±17[a]	4,996±678	2,680±899[b]
P30	297±27	289±35[b]	5±1	8±4[b]	119±11	76±11[a]	5,017±504	3,105±987[b]
P50	295±13	289±26[b]	6±1	7±2[b]	105±3	86±15[a,b]	4,629±215	3,515±337[b]
M + P50	297±222	262±18[a,b]	6±1	13±2[b]	102±16	59±12[c]	4,989±250	2,448±187[c]

Data are expressed as the mean ± SD. [a]P<0.05 vs. N. [b]P<0.05 vs. IR. [c]P<0.05 vs. P50. T1, end of equilibration; T3, end of reperfusion; LVED, left ventricular end-diastolic pressure; LVDP, left ventricular developed pressure; HR, heart rate; +dP/dtmax, maximal rate of rise in blood pressure in the ventricular chamber; N normal; IR, ischemia-reperfusion; MPG, N-(2-mercaptopropionyl)-glycine; P10, 10 μmol/l pinacidil; P30, 30 μmol/l pinacidil; P50, 50 μmol/l pinacidil.

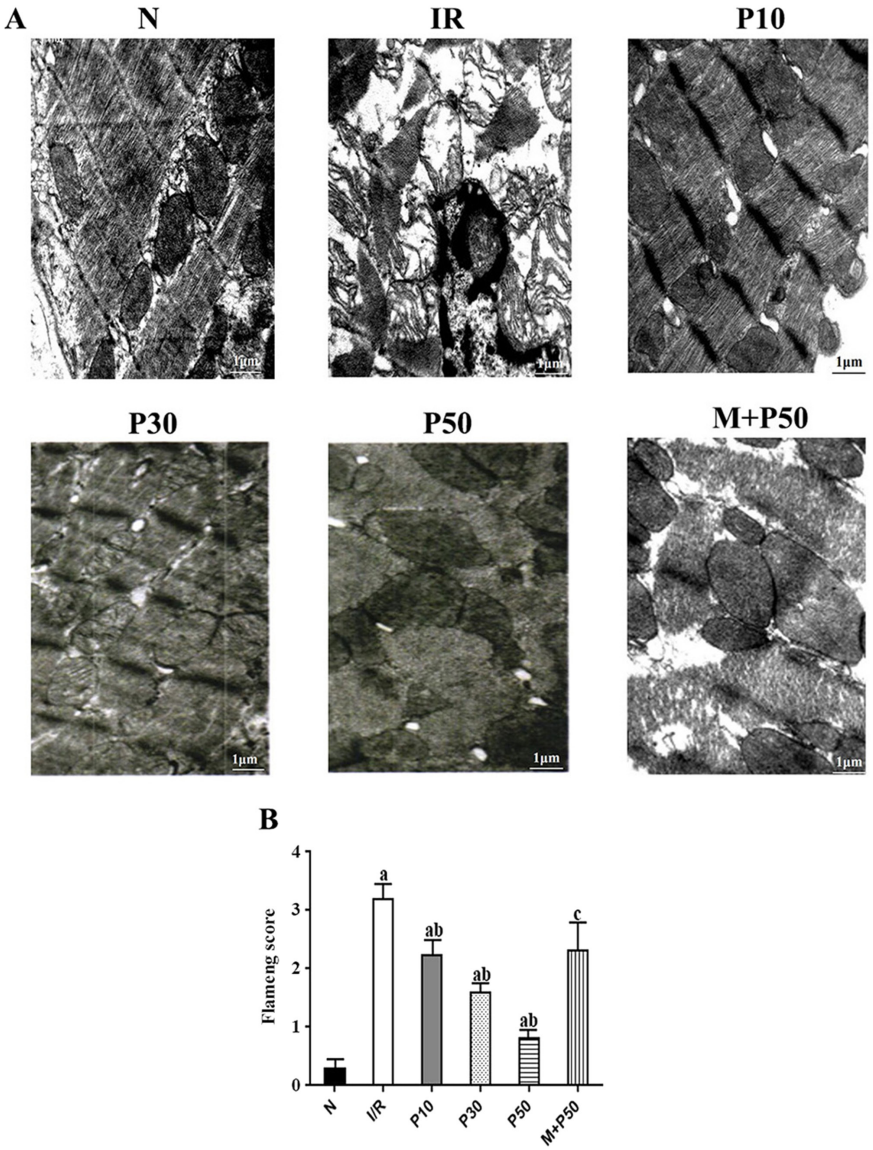

Figure 2. Myocardial morphology. (A) Ultrastructure of isolated rat hearts based on transmission electron microscopy at T3. (B) Mitochondrial damage score in each group at T3. The more severe the damage, the higher the score. Damage in the IR group was the most severe and damage in the P50 group was the least severe. Data were analyzed via Kruskal-Wallis and post hoc Dunn's test. [a]P<0.05 vs. N. [b]P<0.05 vs. IR. [c]P<0.05 vs. P50. T3, end of reperfusion; N, normal; IR, ischemia-reperfusion; P10, 10 μmol/l pinacidil; P30, 30 μmol/l pinacidil; P50, 50 μmol/l pinacidil.

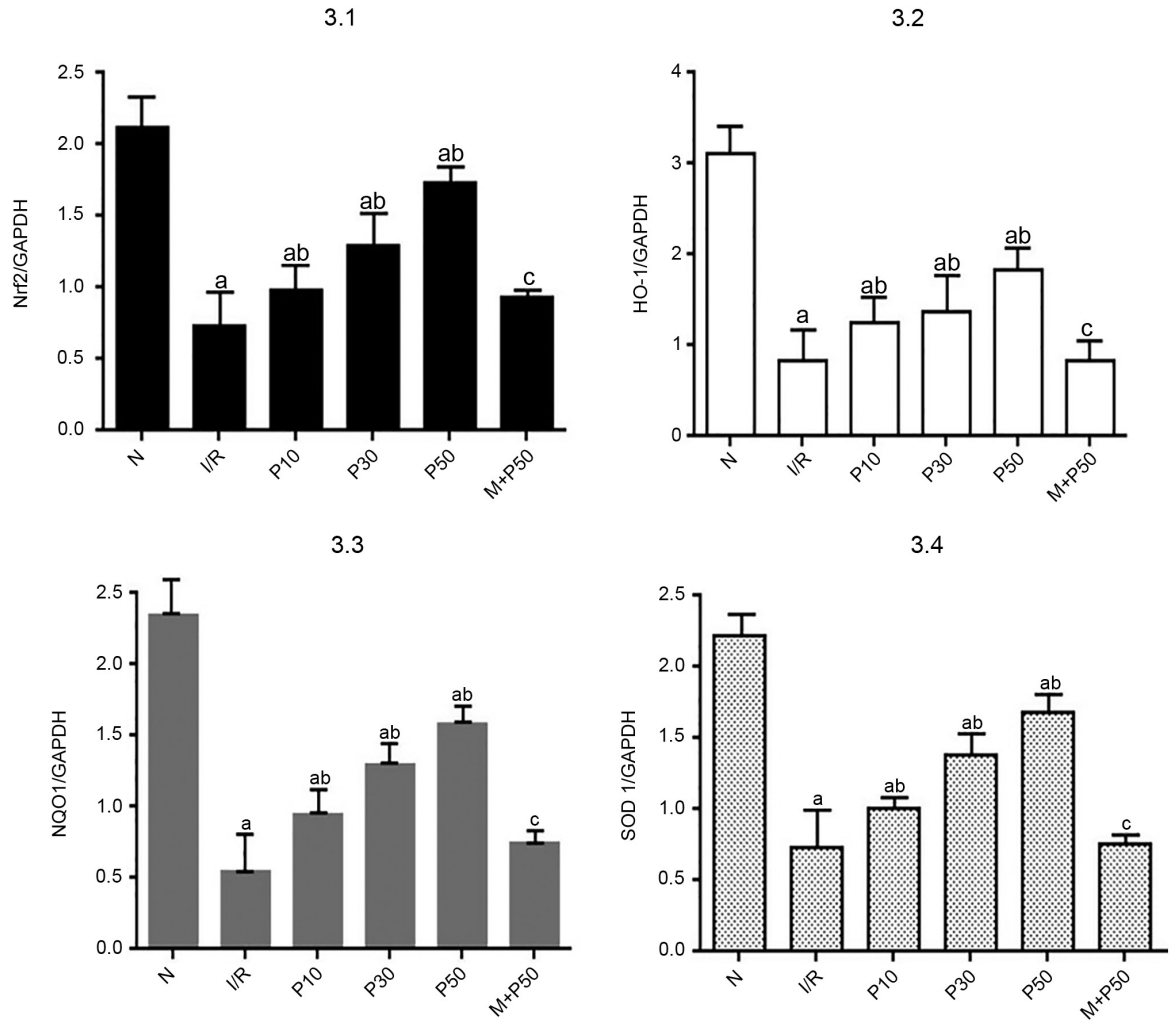

Figure 3. Gene expression levels in isolated rat hearts at T3. Nrf2 pathway-associated mRNA expression levels were lowest in the IR group. The P50 group exhibited the highest mRNA expression levels. [a]P<0.05 vs. N. [b]P<0.05 vs. IR. [c]P<0.05 vs. P50. Data are presented as the mean ± SD (n=3) and were analyzed by one-way ANOVA followed by Bonferroni's correction. T3, end of reperfusion; Nrf2, nuclear factor-E2 related factor 2; IR, ischemia-reperfusion; P10, 10 μmol/l pinacidil; P30, 30 μmol/l pinacidil; P50, 50 μmol/l pinacidil; N, normal; HO-1, heme oxygenase 1; NQO1, NADH-quinone oxidoreductase-1; SOD1, superoxide dismutase 1.

the P50 group. The relative expression levels in the M + P50 group were lower compared with in the P50 group.

Western blot analysis of relative protein expression levels of Nrf2, HO-1, NQO1 and SOD-1 in myocardial tissue at T3. At T3, the expression levels of each protein in the IR group were significantly lower compared with the N group (Fig. 4). The relative expression levels of Nrf2, HO-1, NQO1 and SOD-1 protein were higher in the P10, P30 and P50 groups compared with the IR group. The protein expression levels were highest in the P50 group.

Effects of different concentrations of pinacidil on ROS in rat myocardial tissue. At T2, ROS content in the IR group was the highest. The ROS content of the P10, P30 and P50 groups was significantly lower compared with the IR group (Table II).

The P10 group had the lowest ROS level and the P50 group had the highest ROS level. Until the end of reperfusion, the amount of ROS in the IR group was high but the ROS levels in the P10, P30 and P50 groups decreased over time. The P10 and P50 groups had the highest and lowest ROS contents, respectively. The P10, P30 and P50 groups exhibited lower ROS values at T3 compared with T2. The P50 group exhibited the lowest ROS content at the end of reperfusion (Table III; Fig. 5).

In summary, each concentration of pinacidil was positively associated with relative expression levels of Nrf2, HO-1, NQO1 and SOD1 at T2 but negatively associated at T3. The ROS levels in the P10 group were lowest and those in the P50 group were highest at T2; however, at T3, ROS levels in the P10 group were highest, while those in the P50 group were lowest.

Discussion

Timely and effective reperfusion measures are necessary to save ischemic myocardial tissue (30). However, reperfusion can trigger MIRI, which typically manifests in the early stages of reperfusion and directly induces cardiomyocyte apoptosis or death. The mechanism involves ROS production (31,32), anaerobic metabolic accumulation (33), increased transmembrane osmotic gradient loading, Na^+-K^+ ATPase activation and mPTP opening. ROS production first occurs in the early

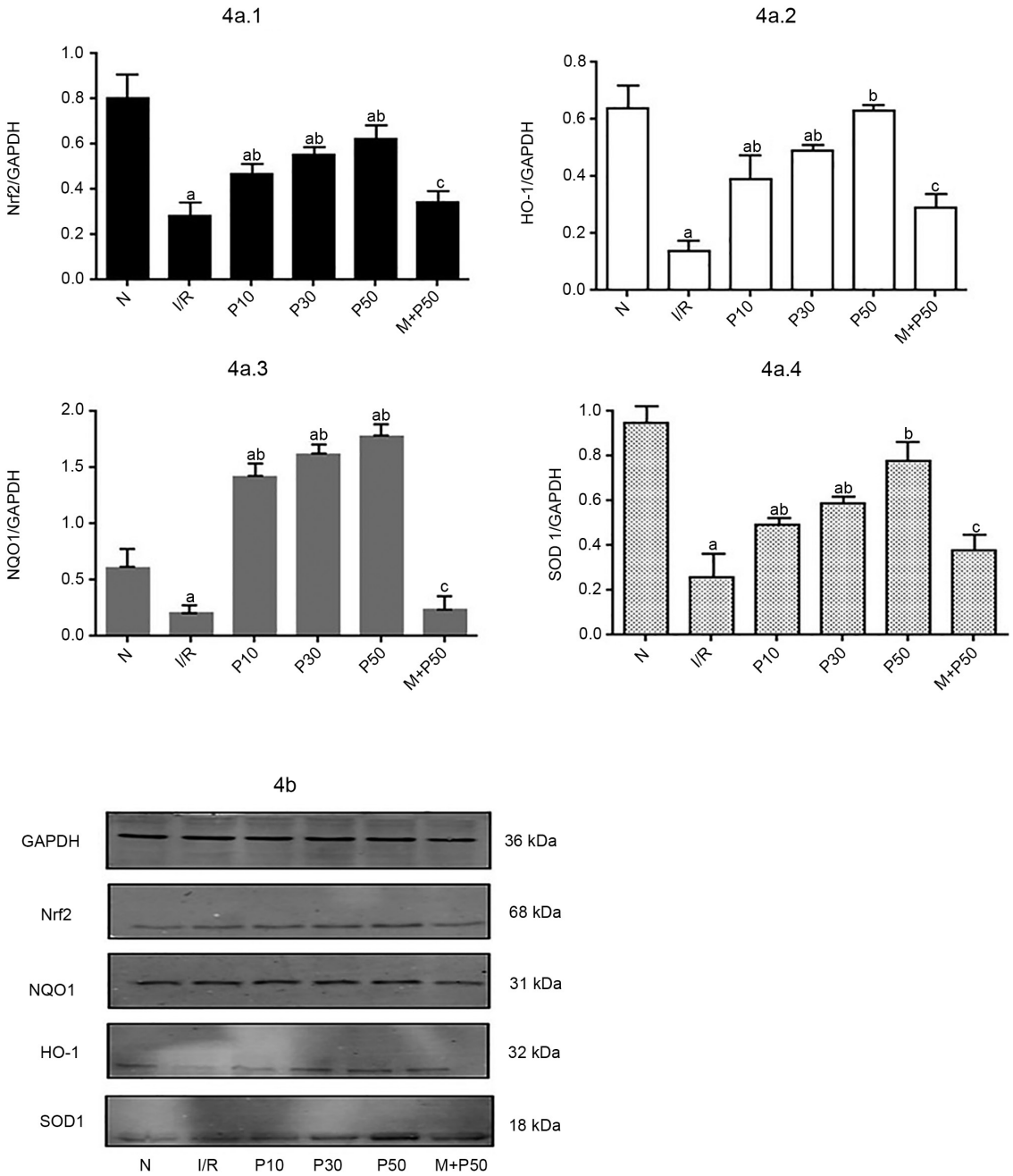

Figure 4. Protein levels in isolated rat hearts at T3. (A) Changes in relative expression levels of Nrf2, NQO1, HO-1 and SOD1. (B) Western blotting was performed to evaluate the protein expression levels of Nrf2, HO-1, NQO1 and SOD1. The IR group exhibited the lowest protein expression levels of Nrf2, HO-1, NQO1 and SOD1. The P50 group exhibited the highest protein expression levels. [a]P<0.05 vs. N. [b]P<0.05 vs. IR. [c]P<0.05 vs. P50. Data are presented as the mean ± SD (n=3). T3, end of reperfusion; Nrf2, nuclear factor-E2 related factor 2; HO-1, heme oxygenase 1; NQO1, NADH-quinone oxidoreductase-1; SOD1, superoxide dismutase 1; IR, ischemia-reperfusion; P10, 10 μmol/l pinacidil; P30, 30 μmol/l pinacidil; P50, 50 μmol/l pinacidil; N, normal.

stages of reperfusion. The earliest stage of reperfusion results in ROS production, which is derived from xanthine oxidase, NADPH oxidase (Nox), mitochondria and unconjugated nitric oxide synthase (34). The present study identified that when the myocardium underwent IR, cardiac function, including HR, +dp/dtmax and LVDP, decreased significantly at the end of reperfusion. Transmission electron microscopy demonstrated cell damage characterized by mitochondrial swelling and vacuolar-like degeneration, with a high Flameng score of 3.19. These results indicate that IR caused severe damage to the myocardium, as well as changes in myocardial morphology and function.

Furthermore, the amount of ROS in the IR group were highest in the early stage or at the end of reperfusion. A study by Chen *et al* (22) confirmed that at the end of reperfusion, MIRI induces significant ROS production, leading to a chain reaction of membrane lipid peroxidation, cell membrane fluidity changes and increased production of the lipid peroxidation by-product malondialdehyde; this increases cellular oxidative stress, leading to myocardial cell death. Han *et al* (35) reported that following IR-induced oxidative stress injury, action potential duration is shortened by IR and ROS production is triggered, leading to mPTP opening and MIRI. Another study demonstrated that myocardial damage caused by IR may be

Table II. ROS levels at T2 and T3 in each group.

Group	T2	T3
N	150.20±25.97	155.20±30.81
IR	330.51±17.73[a]	313.01±35.31[a]
P10	220.01±12.53[a,b]	258.75±9.70[a-c]
P30	241.77±6.35[a,b]	235.45±4.81[a,b]
P50	263.85±9.34[a,b]	228.85±20.99[a-c]

Data are presented as mean ± standard deviation (n=3) and were analyzed by two-way ANOVA, with time as the independent factor, followed by post hoc Bonferroni's correction. [a]P<0.05 vs. N. [b]P<0.05 vs. IR. [c]P<0.05 vs. T2. T2, 5 min after reperfusion, T3, end of reperfusion; ROS, reactive oxygen species; N, normal; IR, ishcemia-reperfusion; P10, 10 μmol/l pinacidil; P30, 30 μmol/l pinacidil; P50, 50 μmol/l pinacidil.

Table III. Association between ROS content and relative expression levels of Nrf2 gene and protein at T3 (n=9).

Group (sample)	ROS levels at T3, U/ml	Nrf2 mRNA	Nrf2 protein
P10			
(1)	249.05	1.10	0.54
(2)	258.75	0.98	0.47
(3)	268.45	0.86	0.40
P30			
(4)	235.64	1.58	0.63
(5)	240.45	1.29	0.55
(6)	245.26	1.00	0.47
P50			
(7)	207.86	1.79	0.69
(8)	228.85	1.73	0.62
(9)	249.84	1.67	0.55

Each measurement was taken from three samples per group. T3, end of reperfusion; ROS, reactive oxygen species; Nrf2, nuclear factor-E2 related factor 2; P10, 10 μmol/l pinacidil; P30, 30 μmol/l pinacidil; P50, 50 μmol/l pinacidil.

due to activation of mitoKATP, which promotes autophosphorylation of ROS products (36). The autophosphorylation of ROS products can result in sustained opening of mitoKATP, which aggravates MIRI (37). These results are consistent with those of the present study.

Pinacidil, a non-selective KATP opener, causes mitochondrial membrane depolarization, decreases transmembrane potential difference, weakens Ca^{2+} internal flow, promotes fatty acid oxidation and maintains ATP levels in cardiomyocytes. The integrity of cardiomyocytes and mitochondrial membranes is maintained to exert myocardial protection (38,39). According to Yang *et al* (9), pinacidil could relieve the MIRI, not only in cardiac function, mitochondrial respiratory function, ATP level and myocardial enzyme content, but also caused myocardial ultrastructure by improving the morphology of muscle fibers.

MPG is a thiol compound with ROS scavenging properties and exerts a protective effect on irreversible and reversible RI (40). In 2004, MPG was approved by the FDA for clinical oral prophylactic treatment (41). Fantinelli *et al* (42) demonstrated that MPG protects hypertrophic myocardium in rats, prevents MIRI, decreases infarct size and oxidative stress, improves myocardium following ischemia and promotes recovery of vascular function.

Ihnken *et al* (43) demonstrated that MPG, as an antioxidant, provides the same protection as coenzyme Q10, allopurinol and arachidonic acid; in dogs during cardiopulmonary bypass, it removed nitrite and harmful substances and served a necessary role in myocardial protection. MPG also decreases the degree of mitochondrial swelling caused by 12.5 mM sodium lactate and 1 mM phenoxide, removes free radicals generated by Na^+ overload in the cytoplasm, prevents free radical attacks, and decreases MIRI. Our previous study (9) confirmed that PPC at a concentration of 50 mmol/l improves cardiac function, decreases myocardial infarct size, maintains mitochondrial structure stability, promotes Nrf2, SOD1, NQO1 and HO-1 expression levels, decreases MIRI and exerts myocardial protection. However, the study did not investigate whether the myocardial protective effects of pinacidil are concentration-dependent or the association between pinacidil and ROS. Therefore, the present study aimed to determine whether different amounts of ROS could affect the expression levels of Nrf2, NQO1, SOD1 and HO-1 to serve a role in alleviating MIRI.

The Nrf2/ARE signaling pathway, which includes HO-1, NQO1 and SOD1, is the regulatory center of the endogenous antioxidant system of the myocardium and serves an important role in anti-MIRI (44). A previous study confirmed that IPO activates Nrf2 and is associated with antioxidant enzymes, such as SOD1, to decrease MIRI (45). Similar to SOD1, NQO1 is expressed at low levels under normal conditions, but oxidative stress, such as IR, promotes expression and increases ROS clearance of NQO1 (46). NQO1 also serves a protective role in renal (47) and cerebral ischemia (48). According to Freixa *et al* (49), β-naphthoflavone increases NQO1 expression, which attenuates cardiomyocyte apoptosis induced by doxorubicin, and enhances the protective effect of progesterone. HO-1 is an endogenous antioxidant that plays a key role in maintaining mitochondrial biochemical function. Previous studies have confirmed that IPO (9,22,50) or drug post-conditioning increases the relative mRNA and protein expression levels of HO-1 to exert anti-MIRI effects. These aforementioned studies confirmed that the expression levels of Nrf2, NQO1, SOD1 and HO-1 increase following MIRI to decrease myocardial oxidative stress and exert a myocardial protective effect.

In the present study, the production of ROS at T2 increased gradually with increased pinacidil concentration; ROS production in the P10 group was the lowest, while that in the P50 group was the highest. In addition, owing to the difference in levels of ROS, the relative mRNA and protein expression levels of Nrf2, NQO1, SOD1 and HO-1 also differed. The P10 group exhibited the lowest ROS content and protein expression levels of Nrf2 and its associated antioxidants;

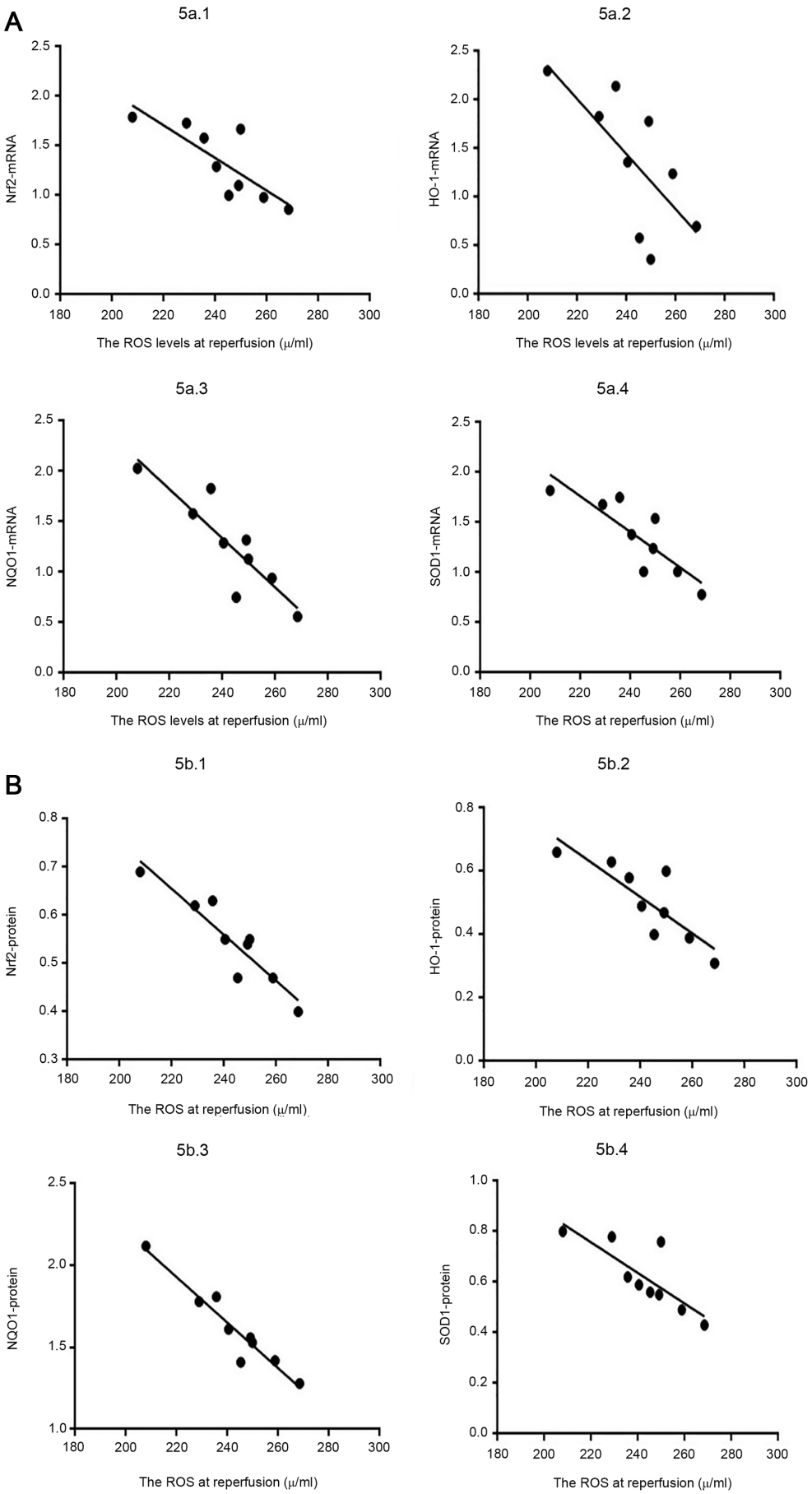

Figure 5. Scatter plots of ROS and Nrf2 gene and protein levels at T3 with different concentrations of pinacidil. Following pinacidil treatment (at concentrations of 10, 30 and 50 μmol/l), ROS production was negatively linearly correlated with (A) mRNA and (B) protein expression levels of Nrf2 mRNA at T3. T3, end of reperfusion; Nrf2, nuclear factor-E2 related factor 2; ROS, reactive oxygen species.

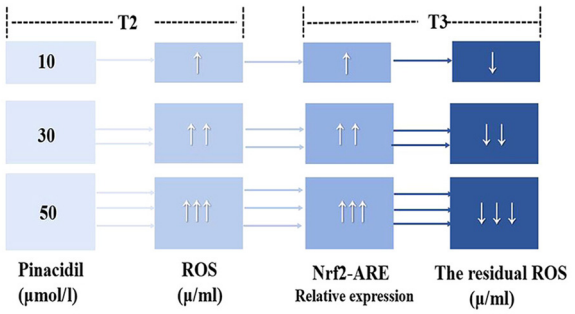

Figure 6. Mechanism of different concentrations of pinacidil postconditioning in the rat cardiac Nrf2-ARE signaling pathway is associated with ROS. Nrf2, nuclear factor-E2 related factor 2; ARE, antioxidant responsive element; ROS, reactive oxygen species; T2, 5 min after reperfusion; T3, end of reperfusion. Different numbers of arrows represent the magnitude of change.

thus, the anti-MIRI effect was weak. Transmission electron microscopy revealed mitochondrial swelling and Z line; a high Flameng score was also noted. By contrast, the ROS content in the P50 group was the highest and the expression levels of Nrf2, SOD1 and NQO1 were also significantly increased at T2. The mitochondrial structure was intact, there was no dissolution or rupture, and the Flameng score was significantly decreased. Paul *et al* (51) reported that by altering ROS levels to activate Nrf2, increased expression of Nrf2 activates the Notch pathway to stimulate self-renewal of human airway basal stem cells, which, in turn, initiate antioxidant processes and eliminate high intracellular ROS levels to maintain a stable environment. This regulation of ROS to regulate Nrf2-pulmonary stem cell function mediated by anti-oxidation is important for stem cell biology, lung injury repair and cancer (51). High expression levels of Nrf2 also induce rapid enzymatic modification, excretion of chemical carcinogens and ROS quenching, and regulate the expression levels of associated antioxidant proteins, such as HO-1 and SOD1, to repair oxidative damage and prevent cancer (52). Similar regulatory features have also been reported in studies by Kensler *et al* (53), Ma (54), Jaramillo and Zhang (55) and Harder *et al* (56).

The present study investigated the effect of high expression levels of Nrf2, HO-1, NQO1 and SOD1 on ROS. The present study found that at T2, the amount of ROS in the P10 group was the lowest, and the expressions of Nrf2, HO-1, NQO1 and SOD1 decreased until T3, at which point the remaining ROS increased. ROS content of the P50 group was highest at T2, although still lower than that of the IR group, and the expression levels of Nrf2, HO-1, NQO1 and SOD1 increased; the ROS content was the lowest at T3. Briefly, at T3, the relative mRNA and protein expression levels of Nrf2, HO-1, NQO1 and SOD1 were negatively linearly correlated with ROS content. This may be because in the early stage of reperfusion, PPC with 10 μmol/l pinacidil resulted in less ROS generation and activated the expression of antioxidant proteins via its phase II detoxification enzyme downstream of the Nrf2 and Nrf2-ARE pathways to a lesser extent (57). The ability to eliminate ROS during reperfusion is limited, which may have resulted in a higher ROS content in the P10 group at the time of reperfusion. Low ROS concentration functions as a signaling molecule that serves different biological roles and determines cell fate by regulating transcription factors of different redox reactions (58); the expression of NQO1, HO-1 and SOD1 genes were all affected by low ROS concentrations, and these genes could alleviate the effect of oxidative stress and toxins (59). This supports the conclusion that low-dose ROS is a signaling molecule that activates the Nrf2-ARE pathway and participates in PPC myocardial protection. The highest concentration of pinacidil used in the present study (50 μmol/l) stimulated greater production of ROS at T2 and activated Nrf2 and its downstream antioxidant proteins, such as HO-1, NQO1 and SOD1, to a greater extent. High expression levels of antioxidant proteins are associated with the elimination of a large amount of ROS molecules produced during reperfusion and therefore exert greater protective effects. Therefore, the ROS concentration in the P50 group was lowest at T3 and the degree of myocardial damage was least severe. Furthermore, the mitochondrial structure was found to be intact. This may be because when ROS are released, the uncoupling of Nrf2 and inhibitory protein kelch-like ECH-associated protein 1 causes Nrf2 to be transferred into the nucleus and bind to ARE to form a heterodimer. The cis-reactive ARE is recognized, which encodes downstream antioxidant protein and phase II detoxification enzyme gene expression, such as glutathione S-transferases, glutathione synthetase, HO-1, NQO1 and SOD1 (32). ARE enhances the antioxidant capacity of tissue, protects tissue from toxic substances and serves an important role in antitumor, anti-inflammatory and anti-apoptotic responses (60).

In the present study, following the application of the ROS scavenger MPG immediately after reperfusion, the degree of myocardial ultrastructural damage and overall cardiac function damage were more severe in the M + P50 group compared with the P50 group and the expression levels of Nrf2 and its downstream genes, such as HO-1, SOD1 and NQO1, were significantly lower in the M + P50 group compared with the P50 group. ROS scavenger may decrease expression levels of genes and proteins, such as Nrf2, HO-1 and SOD1, and downstream regulators, and regulate MIRI by antioxidant proteins and phase II detoxification enzymes, thereby eliminating PPC myocardial protection. This indicates that ROS is an important signaling molecule that activates the Nrf2-ARE pathway and confers protection in PPC. In addition, our previous study aimed to improve the anti-MIRI effect of Nrf2-ARE by increasing pinacidil to 100 μmol/l in rat cardiomyocyte experiments (61). However, the relative expression levels of the genes and proteins did not show a continued increase and myocardial protection was not enhanced (61). The present study further demonstrated that 50 μmol/l pinacidil is the optimal concentration to activate the Nrf2-ARE pathway and decrease MIRI to exert a protective effect.

At T2, the P10 group had the lowest ROS content and the P50 group had the highest ROS content. At T3, the expression levels of Nrf2 and its downstream antioxidant proteins in the P10 group were lowest and the ROS content was higher. The P50 group exhibited the highest expression of Nrf2 and its downstream antioxidant proteins, but lower ROS content. The reason may be that, at T2, 10 μmol/l pinacidil produced less ROS and activated the expression of antioxidant proteins and

phase II detoxification enzymes downstream of the Nrf2 and Nrf2-ARE pathways to a lesser extent. The ability to remove ROS was also small ROS content in the P10 group was still high at T3. Additionally, 50 μmol/l pinacidil produced a higher concentration of ROS and activated expression of antioxidant proteins and phase II detoxification enzymes downstream of the Nrf2 and Nrf2-ARE pathway to a greater extent; the ability to remove ROS also increased so, at T3, the P50 group exhibited lower ROS content.

The higher the pinacidil concentration and expression levels of Nrf2, HO-1, NQO1 and SOD1, the greater the ability to resist MIRI at T3 and the lower the ROS content. Conversely, lower Nrf2 expression levels are associated with decreased ability to resist MIRI and higher ROS content at the end of reperfusion (Fig. 6).

In conclusion, PPC (30-50 μM) promoted the formation of ROS at T2, activated the Nrf2-ARE signaling pathway, regulated the expression of downstream antioxidant proteins and alleviated MIRI in rats. At 50 μM, pinacidil postconditioning produced the most ROS and exhibited the best myocardial protection. The present study may provide an experimental basis for the clinical application of pinacidil in cardiac surgery, coronary artery bypass or percutaneous coronary intervention surgery to decrease MIRI.

Acknowledgements

The authors would like to thank the Key Laboratory of Anesthesia and Organ Protection in Guizhou Province for providing the laboratory.

Funding

The present study was supported by the National Natural Science Foundation of China (grant no. 30960366).

Availability of data and materials

All data used and/or analyzed during the study are available from the corresponding author on reasonable request.

Authors' contributions

WC and HYW participated in the conception and design of the experiments. MYD was involved in drafting the primary manuscript and revising it. WC, MYD, YW and WJZ and TY made substantial contributions to the acquisition of data and interpretation of the data. HYW and TY were involved in revising the manuscript critically for important intellectual content. WC, MYD, HYW, YW, WJZ and TY confirm the authenticity of the raw data in this study. Each author participated sufficiently in the work to take public responsibility for appropriate portions of the content. All authors read and approved the final manuscript.

Ethics approval and consent to participate

The present experiment was approved by document No. 36 of the Animal Ethics Review at The Affiliated Hospital of Zunyi Medical University in 2016. The use and processing of animals was in accordance with the Guide for the Care and Use of Laboratory Animals, published by the National Institute of Health (NIH Publication 88.23, revised 1996).

Patient consent for publication

Not applicable.

Competing interests

The authors declare that they have no competing interests.

References

1. Zhao ZQ, Corvera JS, Halkos ME, Kerendi F, Wang NP, Guyton RA and Vinten-Johansen J: Inhibition of myocardial injury by ischemic postconditioning during reperfusion: Comparison with ischemic preconditioning. Am J Physiol Heart Circ Physiol 285: H579-H588, 2003.
2. Hao M, Zhu S, Hu L, Zhu H, Wu X and Li Q: Myocardial ischemic postconditioning promotes autophagy against ischemia reperfusion injury via the Activation of the nNOS/AMPK/mTOR Pathway. Int J Mol Sci 18: 614, 2017.
3. Zhang L, Cao S, Deng S, Yao G and Yu T: Ischemic postconditioning and pinacidil suppress calcium overload in anoxia-reoxygenation cardiomyocytes via down-regulation of the calcium-sensing receptor. PeerJ 4: e2612, 2016.
4. Foster MN and Coetzee WA: KATP channels in the cardiovascular system. Physiol Rev 96: 177-252, 2016.
5. Cohen MV and Downey JM: Signalling pathways and mechanisms of protection in pre- and postconditioning: Historical perspective and lessons for the future. Br J Pharmacol 172: 1913-1932, 2015.
6. Yang HQ, Foster MN, Jana K, Ho J, Rindler MJ and Coetzee WA: Plasticity of sarcolemmal KATP channel surface expression: Relevance during ischemia and ischemic preconditioning. Am J Physiol Heart Circ Physiol 310: H1558-H1566, 2016.
7. Yaşar S, Bozdoğan Ö, Kaya ST and Orallar HS: The effects of ATP-dependent potassium channel opener; pinacidil, and blocker; glibenclamide, on the ischemia induced arrhythmia in partial and complete ligation of coronary artery in rats. Iran J Basic Med Sci 18: 188-193, 2015.
8. Yang L and Yu T: Prolonged donor heart preservation with pinacidil: The role of mitochondria and the mitochondrial adenosine triphosphate-sensitive potassium channel. J Thorac Cardiovasc Surg 139: 1057-1063, 2010.
9. Yang YH, Zhang Y, Chen W, Wang Y, Cao S, Yu T and Wang H: Pinacidil-postconditioning is equivalent to ischemic postconditioning in defeating cardiac ischemia-reperfusion injury in rat. Eur J Pharmacol 780: 26-32, 2016.
10. Chen X, Han K, Zhang T, Qi G, Jiang Z and Hu C: Grass carp (Ctenopharyngodon idella) NRF2 alleviates the oxidative stress and enhances cell viability through upregulating the expression of HO-1. Fish Physiol Biochem 46: 417-428, 2020.
11. Moon EJ and Giaccia A: Dual roles of NRF2 in tumor prevention and progression: Possible implications in cancer treatment. Free Radic Biol Med 79: 292-299, 2015.
12. Patwardhan J and Bhatt P: Flavonoids derived from abelmoschus esculentus attenuates UV-B induced cell damage in human dermal fibroblasts through Nrf2-ARE pathway. Pharmacogn Mag 12 (Suppl 2): S129-S138, 2016.
13. Loboda A, Damulewicz M, Pyza E, Jozkowicz A and Dulak J: Role of Nrf2/HO-1 system in development, oxidative stress response and diseases: An evolutionarily conserved mechanism. Cell Mol Life Sci 73: 3221-3247, 2016.
14. Bao L, Li J, Zha D, Zhang L, Gao P, Yao T and Wu X: Chlorogenic acid prevents diabetic nephropathy by inhibiting oxidative stress and inflammation through modulation of the Nrf2/HO-1 and NF-κB pathways. Int Immunopharmacol 54: 245-253, 2018.
15. Oh ET and Park HJ: Implications of NQO1 in cancer therapy. BMB Rep 48: 609-617, 2015.
16. Schlager JJ and Powis G: Cytosolic NAD(P)H: (quinone-acceptor)oxidoreductase in human normal and tumor tissue: Effects of cigarette smoking and alcohol. Int J Cancer 45: 403-409, 1990.

17. Peng Q, Lu Y, Lao X, Chen Z, Li R, Sui J, Qin X and Li S: The NQO1 Pro187Ser polymorphism and breast cancer susceptibility: Evidence from an updated meta-analysis. Diagn Pathol 9: 100, 2014.
18. Zhang CY, Ren XM, Li HB, Wei W, Wang KX, Li YM, Hu JL and Li X: Simvastatin alleviates inflammation and oxidative stress in rats with cerebral hemorrhage through Nrf2-ARE signaling pathway. Eur Rev Med Pharmacol Sci 23: 6321-6329, 2019.
19. Feng S, Xu Z, Wang F, Yang T, Liu W, Deng Y and Xu B: Sulforaphane prevents methylmercury-induced oxidative damage and excitotoxicity through activation of the Nrf2-ARE pathway. Mol Neurobiol 54: 375-391, 2017.
20. Zhao T, Chen S, Wang B and Cai D: L-Carnitine reduces myocardial oxidative stress and alleviates myocardial ischemia-reperfusion injury by activating nuclear transcription-related factor 2 (Nrf2)/Heme Oxygenase-1 (HO-1) signaling pathway. Med Sci Monit 26: e923251, 2020.
21. Ma W, Liu M, Liang F, Zhao L, Gao C, Jiang X, Zhang X, Zhan H, Hu H and Zhao Z: Cardiotoxicity of sorafenib is mediated through elevation of ROS level and CaMKII activity and dysregulation of calcium homoeostasis. Basic Clin Pharmacol Toxicol 126: 166-180, 2020.
22. Chen W, Chen XY, Wang Y, Wang HY, Zhou WJ and Yu T: Mechanism of emulsified isoflurane Postconditioning-induced activation of the Nrf2-antioxidant response element signaling pathway during myocardial ischemia-reperfusion: The relationship with reactive oxygen species. J Cardiovasc Pharmacol 73: 265-271, 2019.
23. Huang SY, Chen YC, Kao YH, Hsieh MH, Lin YK, Chen SA and Chen YJ: Redox and activation of protein kinase a dysregulates calcium homeostasis in pulmonary vein cardiomyocytes of chronic kidney disease. J Am Heart Assoc 6: e005701, 2017.
24. Ivanova S, Batliwalla F, Mocco J, Kiss S, Huang J, Mack W, Coon A, Eaton JW, Al-Abed Y, Gregersen PK, *et al*: Neuroprotection in cerebral ischemia by neutralization of 3-aminopropanal. Proc Natl Acad Sci USA 99: 5579-5584, 2002.
25. Hartung T: Comparative analysis of the revised Directive 2010/63/EU for the protection of laboratory animals with its predecessor 86/609/EEC-a t4 report. ALTEX 27: 285-303, 2010.
26. National Research Council (US) Committee for the Update of the Guide for the Care and Use of Laboratory Animals: Guide for the Care and Use of Laboratory Animals. 8th edition. National Academies Press (US), Washington, DC, 2011.
27. Flameng W, Borgers M, Daenen W and Stalpaert G: Ultrastructural and cytochemical correlates of myocardial protection by cardiac hypothermia in man. J Thorac Cardiovasc Surg 79: 413-424, 1980.
28. Li J, Zhou W, Chen W, Wang H, Zhang Y and Yu T: Mechanism of the hypoxia inducible factor 1/hypoxic response element pathway in rat myocardial ischemia/diazoxide post-conditioning. Mol Med Rep 21: 1527-1536, 2020.
29. Livak KJ and Schmittgen TD: Analysis of relative gene expression data using real-time quantitative PCR and the 2(-Delta Delta C(T)) method. Methods 25: 402-408, 2001.
30. Hausenloy DJ, Barrabes JA, Bøtker HE, Davidson SM, Di Lisa F, Downey J, Engstrom T, Ferdinandy P, Carbrera-Fuentes HA, Heusch G, *et al*: Ischaemic conditioning and targeting reperfusion injury: A 30 year voyage of discovery. Basic Res Cardiol 111: 70, 2016.
31. Neri M, Riezzo I, Pascale N, Pomara C and Turillazzi E: Ischemia/Reperfusion injury following acute myocardial infarction: A critical issue for clinicians and forensic pathologists. Mediators Inflamm 2017: 7018393, 2017.
32. Tsutsumi YM, Yokoyama T, Horikawa Y, Roth DM and Patel HH: Reactive oxygen species trigger ischemic and pharmacological postconditioning: In vivo and in vitro characterization. Life Sci 81: 1223-1227, 2007.
33. Granger DN and Kvietys PR. Reperfusion injury and reactive oxygen species: The evolution of a concept. Redox Biol 6: 524-551, 2015.
34. Pisarenko O, Shulzhenko V, Studneva I, Pelogeykina Y, Timoshin A, Anesia R, Valet P, Parini A and Kunduzova O: Structural apelin analogues: Mitochondrial ROS inhibition and cardiometabolic protection in myocardial ischaemia reperfusion injury. Br J Pharmacol 172: 2933-2945, 2015.
35. Han J, Kim N, Park J, Seog DH, Joo H and Kim E: Opening of mitochondrial ATP-sensitive potassium channels evokes oxygen radical generation in rabbit heart slices. J Biochem 131: 721-727, 2002.
36. Zi C, Zhang C, Yang Y and Ma J: Penehyclidine hydrochloride protects against anoxia/reoxygenation injury in cardiomyocytes through ATP-sensitive potassium channels, and the Akt/GSK-3β and Akt/mTOR signaling pathways. Cell Biol Int 44: 1353-1362, 2020.
37. Fan Z, Wen T, Chen Y, Huang L, Lin W, Yin C and Tan W: Isosteviol sensitizes sarcKATP channels towards pinacidil and potentiates mitochondrial uncoupling of diazoxide in guinea pig ventricular myocytes. Oxid Med Cell Longev 2016: 6362812, 2016.
38. Liang W, Chen J, Mo L, Ke X, Zhang W, Zheng D, Pan W, Wu S, Feng J, Song M and Liao X: ATP-sensitive K+ channels contribute to the protective effects of exogenous hydrogen sulfide against high glucose-induced injury in H9c2 cardiac cells. Int J Mol Med 37: 763-772, 2016.
39. Slove S, Lannoy M, Behmoaras J, Pezet M, Sloboda N, Lacolley P, Escoubet B, Buján J and Jacob MP: Potassium channel openers increase aortic elastic fiber formation and reverse the genetically determined elastin deficit in the BN rat. Hypertension 62: 794-801, 2013.
40. Tanonaka K, Iwai T, Motegi K and Takeo S: Effects of N-(2-mercaptopropionyl)-glycine on mitochondrial function in ischemic-reperfused heart. Cardiovasc Res 57: 416-425, 2003.
41. Andreadou I, Iliodromitis EK, Souridis V, Prokovas E, Kostidis S, Zoga A, Dagres N, Tsantili-Kakoulidou A, Kremastinos DT, Mikros E and Anastasiou-Nana M: Investigating the effect of antioxidant treatment on the protective effect of preconditioning in anesthetized rabbits. J Cardiovasc Pharmacol 58: 609-166, 2011.
42. Fantinelli JC, González ALF, Pérez NIA and Mosca SM: Protective effects of N-(2-mercaptopropionyl)-glycine against ischemia-reperfusion injury in hypertrophied hearts. Exp Mol Pathol 94: 277-284, 2013.
43. Ihnken K, Morita K, Buckberg GD, Sherman MP and Young HH: Studies of hypoxemic/reoxygenation injury: Without aortic clamping. VI. Counteraction of oxidant damage by exogenous antioxidants: N-(2-mercaptopropionyl)-glycine and catalase. J Thorac Cardiovasc Surg 110: 1212-1220, 1995.
44. Shanmugam G, Narasimhan M, Tamowski S, Darley-Usmar V and Rajasekaran NS: Constitutive activation of Nrf2 induces a stable reductive state in the mouse myocardium. Redox Biol 12: 937-945, 2017.
45. Buelna-Chontal M, Guevara-Chávez JG, Silva-Palacios A, Medina-Campos ON, Pedraza-Chaverri J and Zazueta C: Nrf2-regulated antioxidant response is activated by protein kinase C in postconditioned rat hearts. Free Radic Biol Med 74: 145-156, 2014.
46. Zai CC, Tiwari AK, Basile V, de Luca V, Müller DJ, Voineskos AN, Remington G, Meltzer HY, Lieberman JA, Potkin SG and Kennedy JL: Oxidative stress in tardive dyskinesia: Genetic association study and meta-analysis of NADPH quinine oxidoreductase 1 (NQO1) and Superoxide dismutase 2 (SOD2, MnSOD) genes. Prog Neuropsychopharmacol Biol Psychiatry 34: 50-56, 2010.
47. Gang GT, Hwang JH, Kim YH, Noh JR, Kim KS, Jeong JY, Choi DE, Lee KW, Jung JY, Shong M and Lee CH: Protection of NAD(P)H:quinone oxidoreductase 1 against renal ischemia/reperfusion injury in mice. Free Radic Biol Med 67: 139-149, 2014.
48. Chen G, Fang Q, Zhang J, Zhou D and Wang Z: Role of the Nrf2-ARE pathway in early brain injury after experimental subarachnoid hemorrhage. J Neurosci Res 89: 515-523, 2011.
49. Freixa X, Bellera N, Ortiz-Pérez JT, Jiménez M, Paré C, Bosch X, De Caralt TM, Betriu A and Masotti M: Ischaemic postconditioning revisited: Lack of effects on infarct size following primary percutaneous coronary intervention. Eur Heart J 33: 103-112, 2012.
50. Limalanathan S, Andersen GØ, Kløw NE, Abdelnoor M, Hoffmann P and Eritsland J: Effect of ischemic postconditioning on infarct size in patients with ST-elevation myocardial infarction treated by primary PCI results of the POSTEMI (POstconditioning in ST-Elevation Myocardial Infarction) randomized trial. J Am Heart Assoc 3: e000679, 2014.
51. Paul MK, Bisht B, Darmawan DO, Chiou R, Ha VL, Wallace WD, Chon AT, Hegab AE, Grogan T, Elashoff DA, *et al*: Dynamic changes in intracellular ROS levels regulate airway basal stem cell homeostasis through Nrf2-dependent Notch signaling. Cell Stem Cell 15: 199-214, 2014.
52. Rojo de la Vega M, Chapman E and Zhang DD: NRF2 and the hallmarks of cancer. Cancer Cell 34: 21-43, 2018.

53. Kensler TW, Wakabayashi N and Biswal S: Cell survival responses to environmental stresses via the Keap1-Nrf2-ARE pathway. Annu Rev Pharmacol Toxicol 47: 89-116, 2007.
54. Ma Q: Role of nrf2 in oxidative stress and toxicity. Annu Rev Pharmacol Toxicol 53: 401-426, 2013.
55. Jaramillo MC and Zhang DD: The emerging role of the Nrf2-Keap1 signaling pathway in cancer. Genes Dev 27: 2179-2191, 2013.
56. Harder B, Jiang T, Wu T, Tao S, Rojo de la Vega M, Tian W, Chapman E and Zhang DD: Molecular mechanisms of Nrf2 regulation and how these influence chemical modulation for disease intervention. Biochem Soc Trans 43: 680-686, 2015.
57. Iguchi K, Saotome M, Yamashita K, Hasan P, Sasaki M, Maekawa Y and Watanabe Y: Pinacidil, a KATP channel opener, stimulates cardiac $Na^{+}/Ca2^{+}$ exchanger function through the NO/cGMP/PKG signaling pathway in guinea pig cardiac ventricular myocytes. Naunyn Schmiedebergs Arch Pharmacol 392: 949-959, 2019.
58. Itoh K, Chiba T, Takahashi S, Ishii T, Igarashi K, Katoh Y, Oyake T, Hayashi N, Satoh K, Hatayama I, *et al*: An Nrf2/small Maf heterodimer mediates the induction of phase II detoxifying enzyme genes through antioxidant response elements. Biochem Biophys Res Commun 236: 313-322, 1997.
59. Satta S, Mahmoud AM, Wilkinson FL, Yvonne AM and White SJ: The role of Nrf2 in cardiovascular function and disease. Oxid Med Cell Longev 2017: 9237263, 2017.
60. Penna C, Rastaldo R, Mancardi D, Raimondo S, Cappello S, Gattullo D, Losano G and Pagliaro P: Post-conditioning induced cardioprotection requires signaling through a redox-sensitive mechanism, mitochondrial ATP-sensitive K+ channel and protein kinase C activation. Basic Res Cardiol 101: 180-189, 2006.
61. Shoujia Y, Haiying W, Tian Y and Xingkui L: The role of Nrf2-ARE pathway in hypoxia/pinacidil post-treatment in reducing hypoxia-reoxygenation injury of rat cardiomyocytes. Chin J Pathophysiology: 1696-1699 +1703, 2013.